Electronic Supplementary Material (ESI) for Nanoscale Advances.

Electronic Supporting Information

Observation of Magnetic Vortex Configuration in Non-stoichiometric Fe_3O_4 Nanospheres

Gopal Niraula[a, b], Denilson Toneto[c], Gerardo F. Goya[d], Giorgio Zoppellaro[e], Jose A. H. Coaquira[b], Diego Muraca[f], Juliano C. Denardin[g*], Trevor P. Almeida[h], Marcelo Knobel[f], Ahmad I. Ayesh[i], and Surender K. Sharma[j,a*]

[a]Department of Physics, Federal University of Maranhao, Sao Luis 65080-805, Brazil
[b]Laboratory of Magnetic Materials, NFA, Institute of Physics, University of Brasilia, Brasilia 70910-900, Brazil
[c]Universidad Central de Chile, 8330601 Santiago, Chile
[d]Instituto de Nanociencia y Materiales de Aragón (INMA), Universidad de Zaragoza, 50018, Zaragoza, Spain
[e]Regional Centre of Advanced Technologies and Materials, Palacky University in Olomouc, Slechtitelu 27, 77900 Olomouc, Czech Republic
[f]Institute of Physics "Gleb Wataghin" (IFGW), University of Campinas (Unicamp), Campinas, SP, Brazil
[g]Universidad de Santiago de Chile (USACH), CEDENNA and Departamento de Física, Santiago 9170124, Chile
[h]SUPA, School of Physics and Astronomy, University of Glasgow, Glasgow, G12 8QQ, UK
[i]Physics Program, Department of Math., Stat. and Physics, College of Arts and Sciences, Qatar University, P. O. Box 2713, Doha, Qatar
[j]Department of Physics, Central University of Punjab, Bathinda, 151401, India

[*]Corresponding author: surender76@gmail.com; ; juliano.denardin@usach.cl

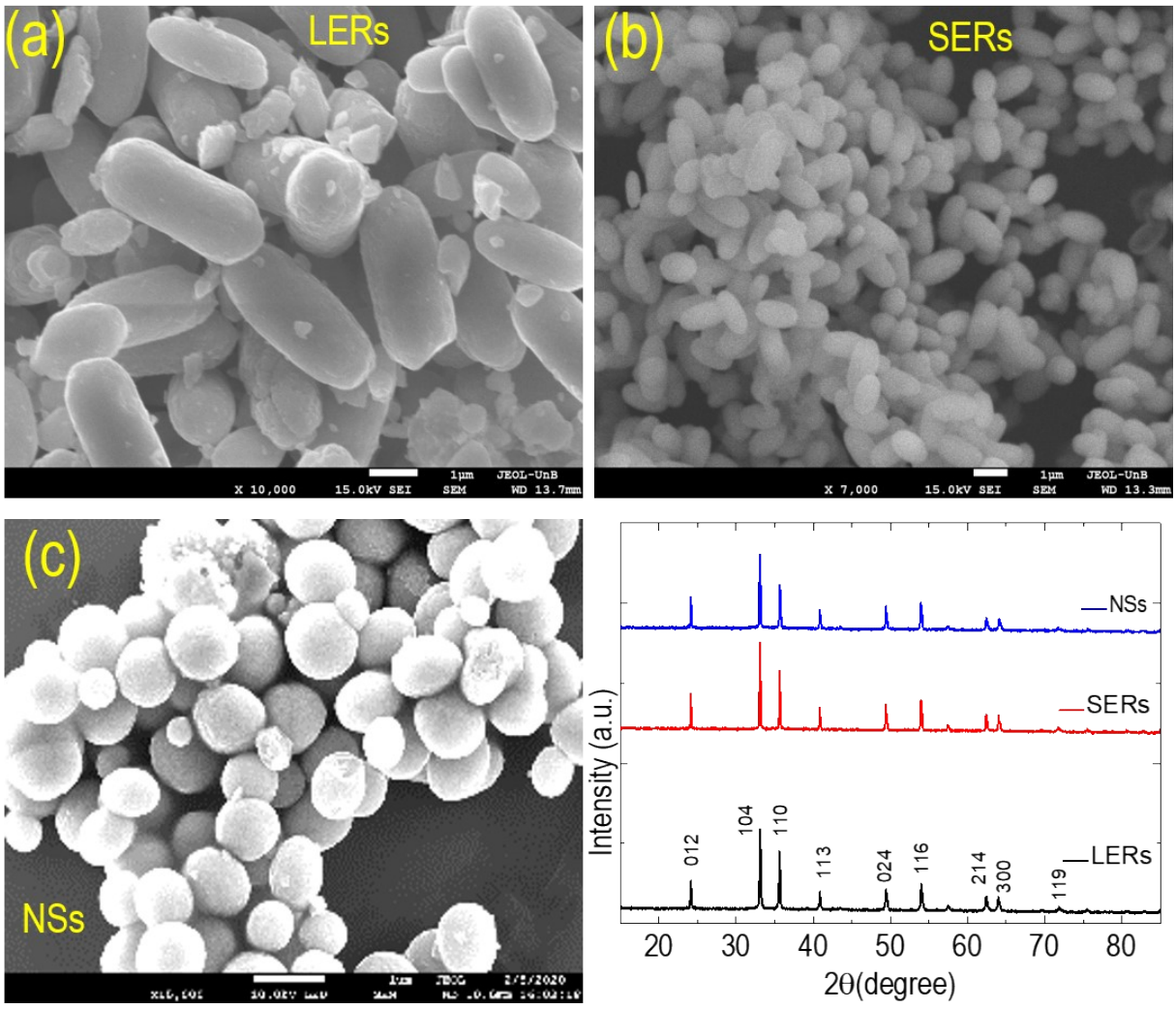

S1: SEM and XRD of α-Fe_2O_3 (JCPDS: 89-0597)

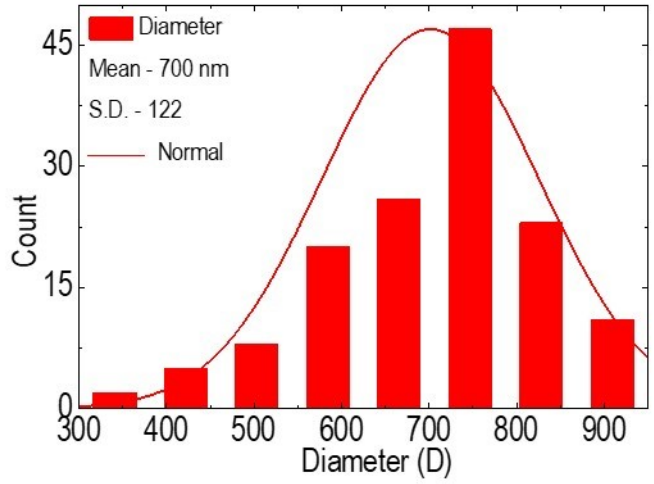

S2: Size distribution of Fe_3O_4 NSs

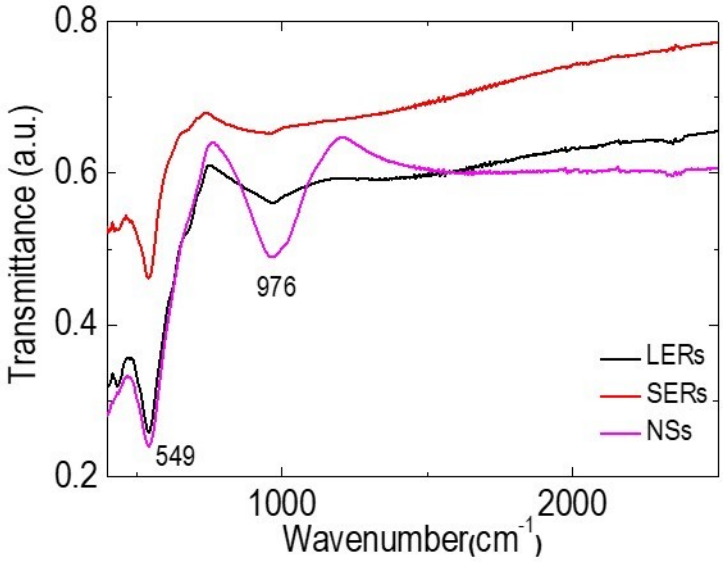

S3: FT-IR of all the samples, i.e. LERs, SERs, and NSs. The detected peaks 549 cm^{-1} and 976 cm^{-1} represent iron oxide (Fe_3O_4 here) and phosphate anion, respectively

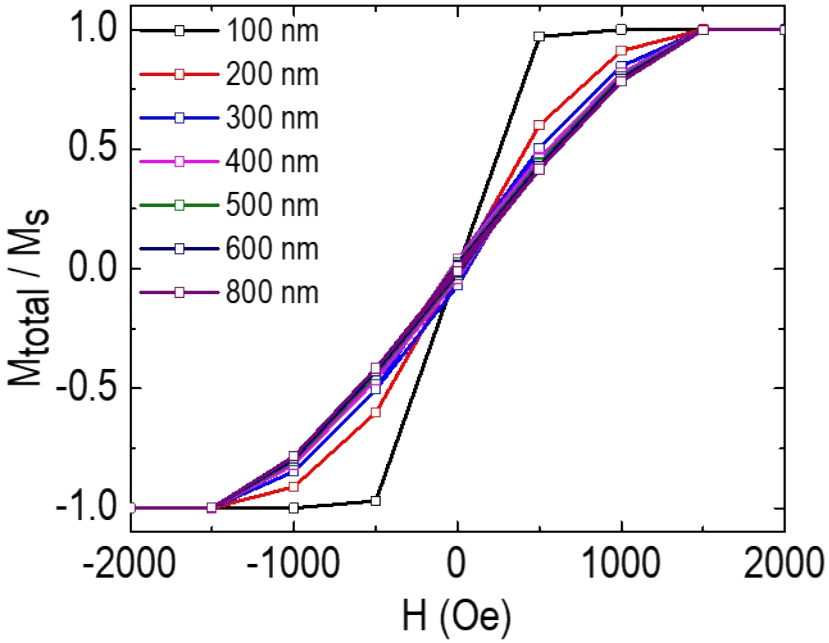

S4: Simulated M-H hysteresis loop varying the size of NSs.

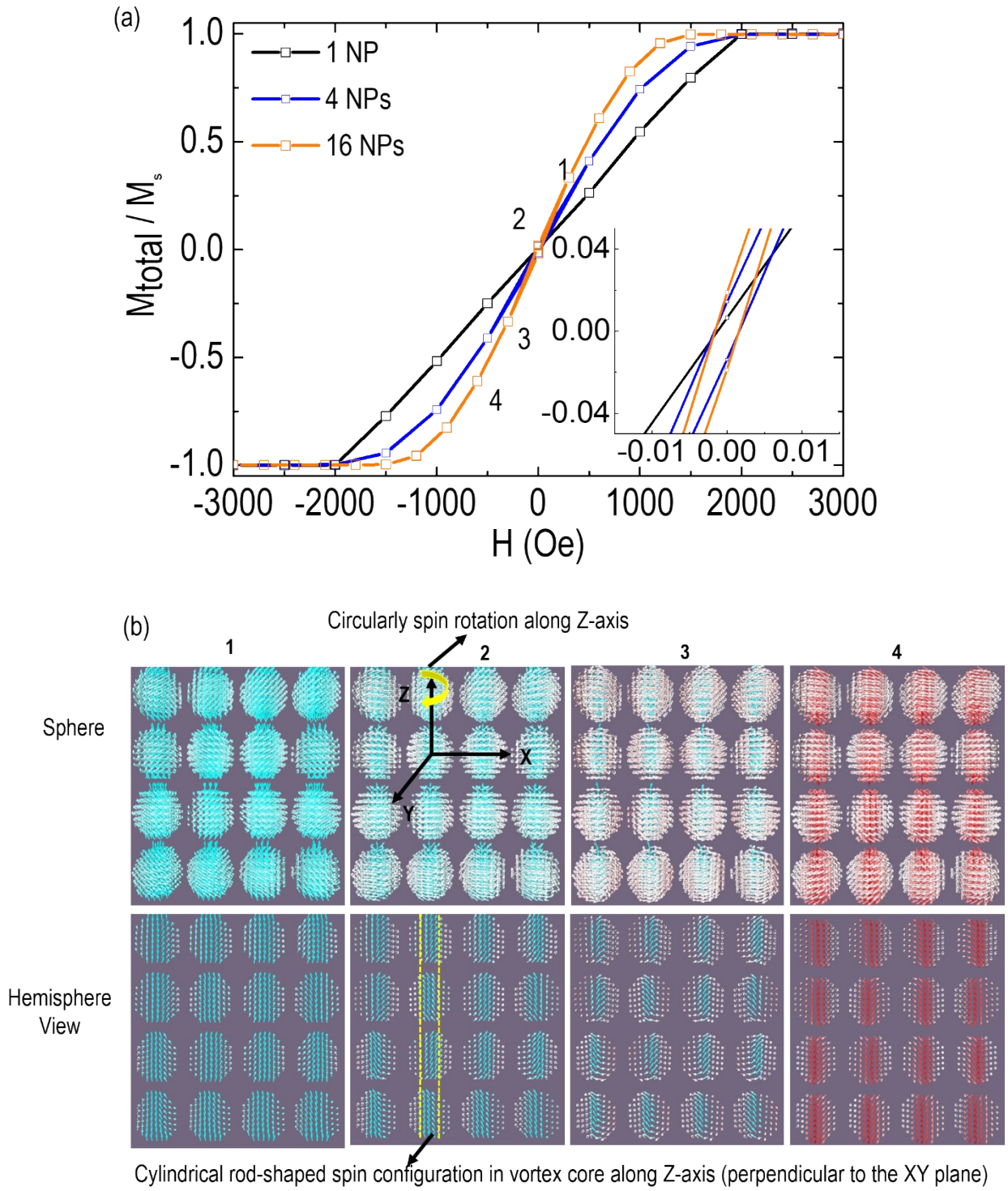

S5: (a) Simulated M-H hysteresis loop varying number of spheres at NSs diameter 700 nm. (b) Upper row contains full-sphere spin configuration rotating around vortex core axis (yellow arrow), i.e., Z-axis (perpendicular) and lower row with corresponding cut-sphere (hemisphere) to show rod-shaped vortex evolution towards Z-axis (parallel yellow dotted line).

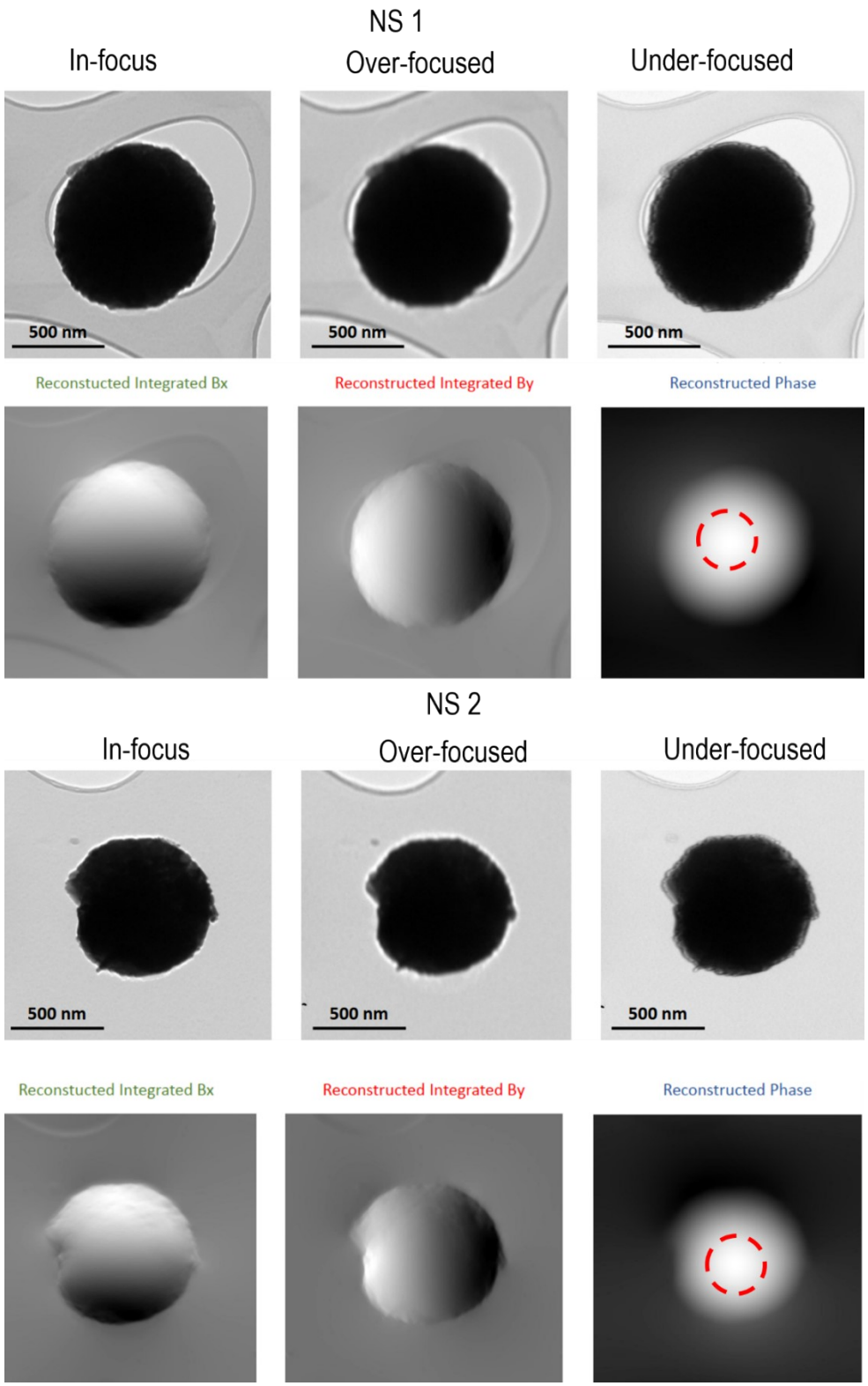

S6: Focus-series of Fresnel contrast imaging technique for two isolated sample NS1 and NS2 and their corresponding reconstructed phase along different field axis.

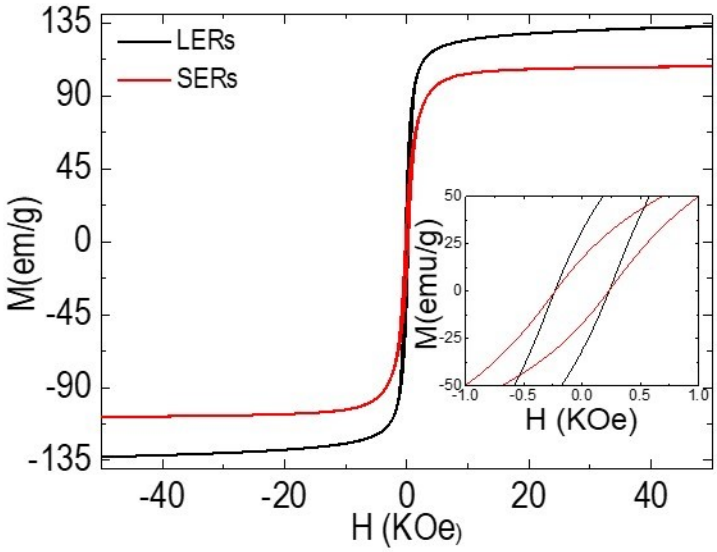

S7: Hysteresis loss of LERs and SERs measured at 300 K applying field of +/- 50 kOe

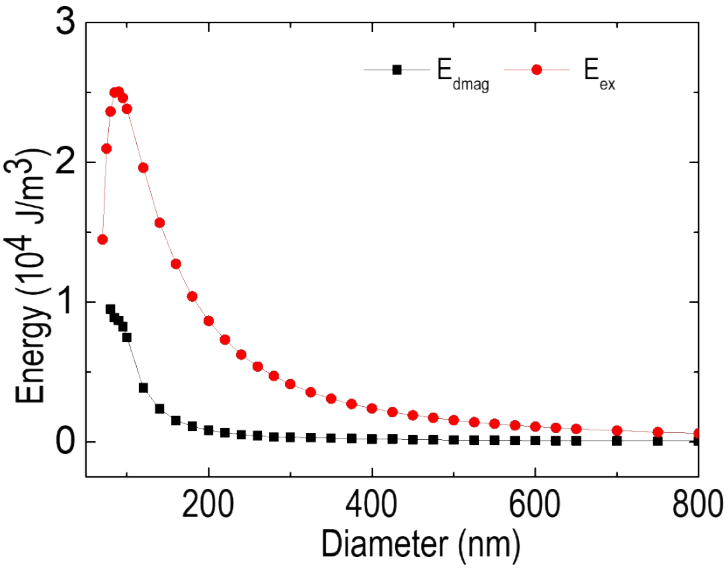

S8: Energy profile of NSs obtained by means of micro-magnetic simulation where magneto-static energy (demagnetizing) is dominated by exchange energy.

Table 1: Comparative study of lattice parameter, phase analysis, and magnetic measurement

Sample	Lattice Parameter (nm) ±0.0005	Phase Analysis				Magnetic Measurement	
		XRD(±1)		Mössbauer(±2)		Verwey Transition Temp. (Tv)	M_S (emu/g)
		Fe_3O_4(%);	Fe^0(%)	Fe_3O_4(%)	Fe^0(%)		
Long Rods	Fe_3O_4 =0.838 Fe^0= 0.286	85.5	14.5	84	16		132
Short rods	Fe_3O_4 =0.838 Fe^0= 0.286	86	12.4	87	11	122 K	108
Sphere	Fe_3O_4 =0.837	100	-	100	-		76

Table 2: Magnetic properties

Sample	Ms (emu/g)	Mr (emu/g)	Hc (Oe)	Mr/Ms
LERs	132	31	232	0.23
SERs	108	17	229	0.16
NSs	70	10	21	0.14

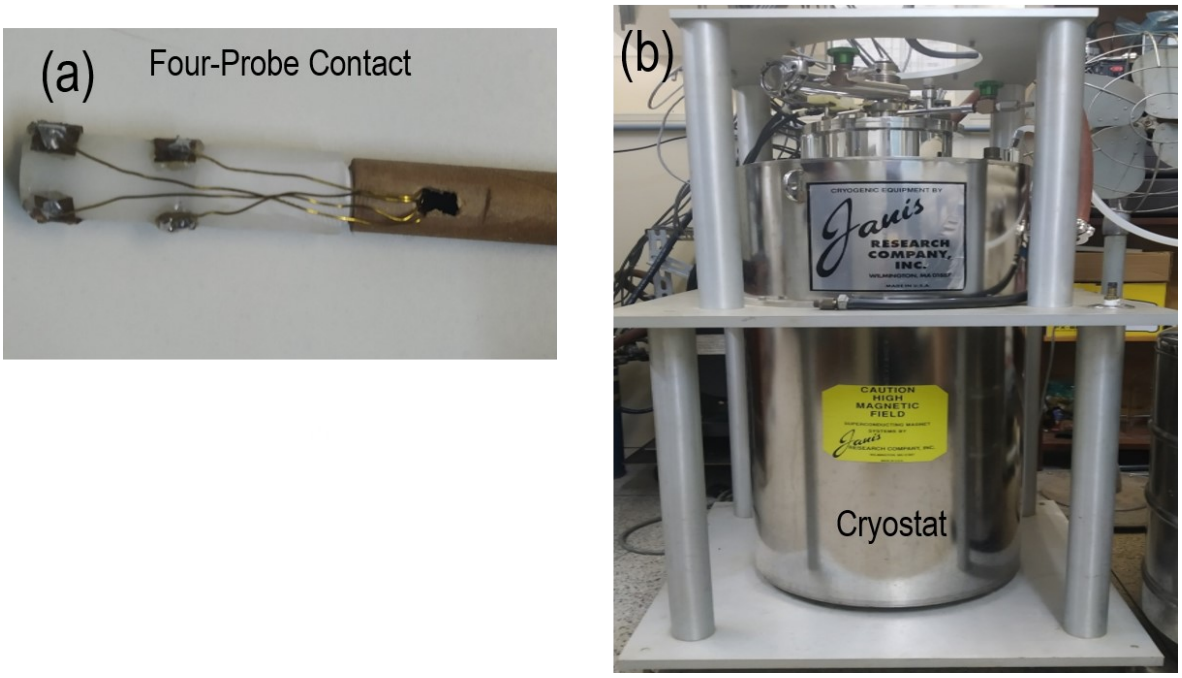

S9: Electrical measurement device. (a) Four-probe contact and (b) Cryostat

Table 3. ^{57}Fe Hyperfine parameters, isomer shift (I.S.), quadrupole splitting (Q.S), hyperfine field (B_{hf}) and spectral area (population distributions) for the diverse iron oxide preparations.

Sample	Phase	site	Hyperfine parameters			
			I.S.(mm/s) ±0.01	Q.S.(mm/s) ±0.01	B_{hf} (T) ±0.1	Population (%) ±2
LERs	Fe_3O_4	A(Fe^{3+})	0.29	-0.07	49.48	18.86
		B (Fe^{3+}, Fe^{2+})	0.69	-0.15	45.70	35.74
		A(Fe^{3+})	0.32	-0.002	49.70	26.54
	Fe		-0.02	0	33.00	18.85
SERs	Fe_3O_4	A(Fe^{3+})	0.32	-0.04	49.64	16.43
		B (Fe^{3+}, Fe^{2+})	0.63	0.07	45.33	33.64
		A(Fe^{3+})	0.32	-0.002	49.70	41.17
	Fe		-0.02	0	32.96	8.8
NSs	Fe_3O_4	A(Fe^{3+})	0.31	-0.064	48.83	55.58
		B(Fe^{2+})	0.79	-0.37	46.52	21.20
		B(Fe^{3+})	0.38	0	47.64	23.22

The obtained hyperfine fitting results for LERs and SERs can be discussed considering possible model of core/shell structure assuming that some sample region in the core obey the bulk Fe_3O_4

composition (i.e., stoichiometric) though the remaining portion are non-stoichiometric at vacancies/defects probably within the shell/surface region, in agreement with previous results reported elsewhere [1]. The presence of stoichiometric Fe_3O_4 in these sample is the signature of the possible Verwey phase transition, which occurs near 120 K [2]. Below the Verwey temperature T_V, the valence states of iron ions in both A- and B-sites are mostly stable, though above T_V an electron exchange among Fe^{2+} and Fe^{3+} ions in octahedral B-sites appears and hence these valence states get unstable, giving rise to changes in many physical properties along with structural change from monoclinic to cubic, in agreement with the clear observation of Verwey phase transition in ZFC curve, shown in Figure 4a.

Moreover, it is well known that magnetic moment (M) per formula unit for the stoichiometric Fe_3O_4 is 'M' =4 μ_B. In the present work, the part of non-stoichiometry in LERs, SERs, and NSs led to the magnetic moment 'M' = 3.76 μ_B with δ = 0.12 and hence can be represented by non-stoichiometric formula $Fe_{2.88}O_4$, 'M' = 3.68 μ_B with δ = 0.14 and represented by $Fe_{2.86}O_4$, and 'M' = 3.52 μ_B with δ = 0.16 and represented by $Fe_{2.88}O_4$ for LERs, SERs, and NSs respectively. The increased number of vacancies and surface effects from LERs to NSs is believed to be due to a rise in concentration of phosphate anions during synthesis.

References

(1) Lyubutin, I. S.; Lin, C. R.; Korzhetskiy, Y. V.; Dmitrieva, T. V.; Chiang, R. K. Mössbauer Spectroscopy and Magnetic Properties of Hematite/Magnetite Nanocomposites. *J. Appl. Phys.* **2009**, *106* (3). https://doi.org/10.1063/1.3194316.

(2) VERWEY, E. J. W. Electronic Conduction of Magnetite (Fe3O4) and Its Transition Point at Low Temperatures. *Nature* **1939**, *144* (3642), 327–328. https://doi.org/10.1038/144327b0.